Decellularized homologous tissue-engineered heart valves as off-the-shelf alternatives to xeno- and homografts

Dijkman, Petra E ; Driessen-Mol, Anita ; Frese, Laura ; Hoerstrup, Simon P ; Baaijens, Frank P T

Abstract: Decellularized xenogenic or allogenic heart valves have been used as starter matrix for tissue-engineering of valve replacements with (pre-)clinical promising results. However, xenografts are associated with the risk of immunogenic reactions or disease transmission and availability of homografts is limited. Alternatively, biodegradable synthetic materials have been used to successfully create tissue-engineered heart valves (TEHV). However, such TEHV are associated with substantial technological and logistical complexity and have not yet entered clinical use. Here, decellularized TEHV, based on biodegradable synthetic materials and homologous cells, are introduced as an alternative starter matrix for guided tissue regeneration. Decellularization of TEHV did not alter the collagen structure or tissue strength and favored valve performance when compared to their cell-populated counterparts. Storage of the decellularized TEHV up to 18 months did not alter valve tissue properties. Reseeding the decellularized valves with mesenchymal stem cells was demonstrated feasible with minimal damage to the reseeded valve when trans-apical valve delivery was simulated. In conclusion, decellularization of in-vitro grown TEHV provides largely available off-the-shelf homologous scaffolds suitable for reseeding with autologous cells and trans-apical valve delivery.

DOI: https://doi.org/10.1016/j.biomaterials.2012.03.015

Decellularized Homologous Tissue-engineered Heart Valves as Off-the-Shelf Alternatives to Xeno- and Homografts

Petra E. Dijkman[a], Anita Driessen-Mol[a*], Laura Frese[b,c], Simon P. Hoerstrup[a,b,c], Frank P.T. Baaijens[a]

[a] Department of Biomedical Engineering, Eindhoven University of Technology, PO Box 513, 5600MB Eindhoven, The Netherlands; [b] Swiss Center for Regenerative Medicine, University Hospital and University Zurich, Moussonstrasse 13 • CH 8091 Zurich, Switzerland; [c] Division of Surgical Research & Clinic for Cardiovascular Surgery, University Hospital Zurich, Raemistrasse 100, CH 8091 Zurich, Switzerland

Short title: Decellularized TEHV

* Corresponding author:

Anita Driessen-Mol,

Department of Biomedical Engineering

Eindhoven University of Technology

GEM-Z 4.110, PO Box 513, 5600 MB Eindhoven, The Netherlands

Phone: + 31 40 2473048

Fax: + 31 40 2447355

a.driessen@tue.nl

Abstract

Decellularized xenogenic or allogenic heart valves have been used as starter matrix for tissue-engineering of valve replacements with (pre-)clinical promising results. However, xenografts are associated with the risk of immunogenic reactions or disease transmission and availability of homografts is limited. Alternatively, biodegradable synthetic materials have been used to successfully create tissue-engineered heart valves (TEHV). However, such TEHV are associated with substantial technological and logistical complexity and have not yet entered clinical use. Here, decellularized TEHV, based on biodegradable synthetic materials and homologous cells, are introduced as an alternative starter matrix for guided tissue regeneration. Decellularization of TEHV did not alter the collagen structure or tissue strength and favored valve performance when compared to their cell-populated counterparts. Storage of the decellularized TEHV up to 18 months did not alter valve tissue properties. Reseeding the decellularized valves with mesenchymal stem cells was demonstrated feasible with minimal damage to the reseeded valve when trans-apical valve delivery was simulated. In conclusion, decellularization of in-vitro grown TEHV provides largely available off-the-shelf homologous scaffolds suitable for reseeding with autologous cells and trans-apical valve delivery.

178 words

Keywords: Heart valve tissue engineering, Tissue regeneration, Scaffold, Decellularization, Retraction, Mesenchymal stem cells.

Introduction

Worldwide, approximately 280.000 valve replacements are performed annually [1]. However, the quest for the ideal heart valve replacement is ongoing as current substitutes, like mechanical and bioprosthetic valves, lack the capability for regeneration and growth. This represents a substantial limitation for long-term durability, especially in children and young adults. Guided tissue generation and tissue engineering of heart valves are proposed to overcome the limitations of the current valve replacements. Both decellularized xenogenic and allogenic heart valves have been used as scaffold material for this purpose with pre-clinical and clinical trials showing promising results [2-6]. However, a drawback in using either xenografts or homografts is the risk for an immunogenic response [7], which may unfavorably impact the long-term graft durability [8]. Graft decellularization is applied to decrease this immunological response, however, it is suggested that a number of inflammatory stimuli are still active within decellularized xenogenic tissue, causing graft failure [9]. In addition, the use of unfixed xenografts carries the risk of disease transmission, such as e.g. Creutzfeldt–Jakob disease [10]. The decellularized homograft (allograft) is therefore a safer option compared to the xenograft. Additionally, the homograft microstructure is favorable regarding survival, proliferation, and differentiation of reseeded cells [11]. However, a major limitation of homografts is their limited availability due to donor shortage, especially regarding small-sized valves.

As alternative to xeno- and homografts, biodegradable synthetic materials have been investigated for tissue engineering [12-15]. These materials are attractive because of their unlimited supply, and the lack of any xenogenic disease transmission and rejection risk. After biodegradation of the scaffold, a completely autologous living valve can be obtained with the capability to adapt, remodel and grow [14].These living tissue-engineered heart valves (TEHV) have shown in-vitro and in-vivo functionality [11,14,16-23]. However, a common observation is retraction of the leaflets, resulting in valvular insufficiency [12,19,22,24-26]. As the observed retraction is mainly cell-mediated, cell removal of TEHV represents a strategy

to reduce retraction of the leaflets. Upon attaining sufficient amounts of extracellular matrix in-vitro, removal of the cells can be realized by a decellularization procedure. Decellularization has been intensively investigated for xeno- and homografts [27]. Although this procedure has been applied to tissue-engineered arteries [28-30], it is to our knowledge, not applied to TEHV. In addition to reducing cell-mediated leaflet retraction, decellularization enables storage and subsequent off-the-shelf availability of the valve replacements.

To overcome the limitations of current valve replacements and tissue-engineered solutions, there is a need for a widely available, unfixed, homologous valve substitute, without the loss of functionality due to leaflet retraction. Therefore, in this study we investigate to decellularize in-vitro grown TEHV based on rapidly degrading synthetic scaffolds and homologous cells. We tested the feasibility of this approach by demonstrating cell removal and analysis of the biomechanical properties and in-vitro functionality. Clinical applicability was evaluated by studying the effect of storage upon the tissue properties of the decellularized TEHV. These off-the-shelf homologous valves can be used as scaffold for guided tissue generation or be reseeded prior to implantation. Non-toxicity and reseeding capacity of the decellularized TEHV with bone-marrow mesenchymal stem cells (MSC) was investigated. In addition, the impact of crimping on the reseeded cells was assessed to demonstrate feasibility of the use of reseeded decellularized TEHV for minimally invasive valve delivery.

Materials and methods

Heart valve tissue engineering

Tri-leaflet heart valve scaffolds (n=15) were fabricated from non-woven polyglycolic-acid meshes (PGA; thickness 1.0 mm; specific gravity 70 mg/cm3; Cellon, Bereldange Luxembourg) and coated with 1.75% poly-4-hydroxybutyrate (P4HB; MW: 1 x 106; TEPHA Inc., Lexington MA USA) in tetrahydrofuran (THF; Fluka (Sigma-Aldrich, St Louis MO USA)). Scaffolds were integrated into radially self-expandable nitinol stents (length=27mm,

OD=25mm (n=9) or OD=30mm (n=6) when fully expanded at 37°C; pfm-AG, Köln Germany). Ovine vascular derived cells (previously characterized to express vimentin, SMemb, and hsp47, and partially α-SMA {Geemen, 2012 317 /id}), expanded in DMEM Advanced (Gibco, Invitrogen, Carlsbad CA USA), supplemented with 10% lamb serum (Gibco, Invitrogen), 1% GlutaMax (Gibco, Invitrogen), and 1% Penicillin-streptomycin (Lonza, Verviers Belgium), were seeded onto the stented heart valve scaffolds ($1.5x10^6$ cells/cm^2, passage 6) using fibrin as cell carrier [13]. After seeding, scaffolds were placed into Diastolic Pulse Duplicator systems for culture in closed configuration [32]. The leaflets were exposed to dynamic strains by applying increasing transvalvular pressure differences that started from 3 mm Hg after 5 days and build up to 15 mm Hg in the 4 following days and kept as such until the fourth week. TE-medium (DMEM Advanced, supplemented with 0.1% lamb serum, 1% GlutaMax, 1% Penicillin-streptomycin, and L-ascorbic acid 2-phosphate (0.25 mg/ml; Sigma-Aldrich)) was replaced every 2 to 3 days. After 4 weeks of culturing, the TEHV were either decellularized (n=12) or analyzed directly as cell-populated controls (n=3).

Decellularization

A decellularization protocol, based on existing protocols [33,34], was applied to the in-vitro grown TEHV (n=12). In short, the TEHV were washed three times in PBS (Sigma-Aldrich) and decellularized overnight via incubation in PBS supplemented with 0.25% Triton X-100 (Merck, Darmstadt Germany), 0.25% sodium deoxycholate (SD, Sigma-Aldrich), and 0.02% EDTA (Sigma-Aldrich) at 37°C. Decellularization was followed by two washing cycles in PBS. Subsequently, TEHV were treated with a nuclease digestion solution of 50-mM TRIS-HCl buffer (Tris (hydroxymethyl)-aminomethan (Merck) pH 8.0, supplemented with 100 U/ml Benzonase® (25 units/µl, Novagen, Madison WI USA) and 1 mmol/l of $MgCl_2$ (Merck)) at 37°C, to remove remaining nucleic remnants. After 5-8 hours the nuclease digestion solution was replaced with a nuclease digestion solution containing 80 U/ml Benzonase® and incubated overnight. Thereafter, the solution was replaced again by a 20 U/ml Benzonase® solution and incubated for 5-8 hours. The TEHV were washed twice in PBS, followed by a

washing cycle with M-199 medium (Gibco, Invitrogen) for more than 24 hours at 4°C to remove cellular remnants. TEHV were washed twice in PBS to remove the medium, sterilized in 70% EtOH (70% ethanol absolute (VWR international S.A.S. Fontenay-Sous-Bois, France) and 30% autoclaved ultrapure water) for 30 minutes, and again washed in sterile PBS. All steps were conducted under continuous shaking. Decellularized TEHV were used for functionality testing (n=6), stored for 18 months in fresh M-199 medium (at 4^{o}C) (n=2), or reseeded with MSC (n=4).

In-vitro valve performance of cell-populated- and decellularized TEHV

Functionality of the cell-populated TEHV and decellularized TEHV was visualized in a custom-built valve tester [35], using a high-speed video camera (MotionScope M-5; IDT, Lommel Belgium). To minimize cell-mediated retraction in the cell-populated TEHV before testing, separation of the fused leaflets was performed within 5 minutes prior to testing. Cell-populated (n=3, ID=23mm) and decellularized (n=4, ID=23mm; n=2, ID=28mm) TEHV were exposed to pulmonary conditions for 20 minutes (peak systolic blood pressure of 30 mmHg; end-diastolic blood pressure of 10 mmHg; 72 bpm). The resulting flow and pressure profiles were measured using flow (Transonic, Ithaca NY USA) and pressure sensors (Becton Dickinson, Temse Belgium). To assess prolonged endurance of the decellularized TEHV, the exposure to pulmonary conditions was continued for 24 hours (n=1, OD=23mm; n=2, OD=28mm). The cell-populated TEHV showed too much regurgitation to perform endurance tests. Measures for regurgitation, effective orifice area (EOA, expressed in percentage of the valve root surface area in order to compare valves with different diameters), and peak systolic pressure gradient were obtained for each tested valve after 20 minutes and 24 hours (if applicable) by averaging these parameters over 10 cycles and compared to those of a porcine aortic bioprosthesis (n=1; ID=23mm; Epic Valve, St. Jude Medical Inc, St. Paul MN USA).

Reseeding decellularized TEHV with mesenchymal stem cells (MSC)

MSC isolation, characterization, and differentiation potential

MSC were isolated from bone marrow of adult sheep by density gradient using standardized protocols [36]. The mononuclear cell fraction was plated out in expansion medium (α-MEM (Gibco, Invitrogen), supplemented with 10% calf serum (Gibco, Invitrogen), 2 mM L – Glutamin (Gibco, Invitrogen), and 1% Penicillin-streptomycin (Lonza)). After 72 hours, the non-adherent cells were discarded and adherent cells were washed gently with medium, cultured for about 14 days, and subsequently stored in liquid nitrogen. One week prior to seeding MSC were thawed and expanded further in growth medium (MSC-medium; α-mem (Gibco, Invitrogen), supplemented with 10% lamb serum (Gibco, Invitrogen), 1% GlutaMax (Gibco, Invitrogen), and 1% Penicillin-streptomycin (Lonza)), which was replaced twice per week.

Cells (passage 2 and 10) were FACS analyzed for MSC cell surface markers CD29, CD44, CD166, Stro-4, CD14, CD45, and CD31 [37]. To induce differentiation into adipocytes and osteocytes, ovine MSC were plated at 1000 cells per cm^2 in multiwall plates. For adipogenic differentiation the basic medium DMEM (Gibco, Invitrogen) was supplemented with 1 µM dexamethasone (Sigma-Aldrich), 120 µM indomethacin (Sigma-Aldrich), 10 µg/ml insulin (Sigma-Aldrich), 2 mM L-glutamine (Gibco, Invitrogen) and penicillin/streptomycin (Gibco, Invitrogen). The osteogenic induction medium contained DMEM supplemented with 10 mM β- glycerophol-2-phosphate (Sigma-Aldrich), 50µM ascorbic acid-2-phosphate (Sigma-Aldrich), 10µm dexamethasone, 2 mM L-glutamine, penicillin/ streptomycin and 10% FCS (Biowest, France). The chondrogenic differentiation was evaluated in a 15 ml conical tube with $2x10^5$ cells/ml in DMEM medium supplemented with 2 mM L-glutamine, 1% FCS, 10 ng/ml TGF-β (Peprotech, USA), 50 µM ascorbic acid and 0.5 µg/ml insulin. During the total differentiation period of 21days all induction media were replaced three times a week. The differentiation cultures were harvested after 21 days, washed in PBS and fixed in 4% Formalin for 1 h before histological analyses. For histological evaluation cells were stained with Oil Red-O (to detect lipid vacuoles), Alizarin Red S (to detect calcium deposits) and Toluidin blue staining (to detect cartilage-specific proteoglycan synthesis).

Reseeding decellularized TEHV with MSC

To show feasibility of the decellularized TEHV as living implant, decellularized TEHV (n=4) were reseeded with ovine bone marrow derived mesenchymal stem cells (MSC; $0.1x10^6$ cells/cm^2, passage 5). In order to create a confluent layer of MSC on the valves, the reseeded valves were cultured in MSC-medium under static conditions for 2 to 3 days until further analysis.

Crimping and cell viability of reseeded decellularized TEHV

To demonstrate the potential of the living TEHV for minimally invasive implantation procedures, simulation of the necessitated crimping procedure was performed with the reseeded decellularized TEHV (n=3), as described previously [22]. After simulation of the crimping procedure cell viability was assessed and compared to the non-crimped control (n=1) by whole-mount staining with cell tracker green CMFDA (CTG; Molecular Probes, the Netherlands) and propidium iodine (PI; Molecular Probes, the Netherlands), as described previously [38]. Visualization was performed with a 2-photon confocal microscope (Laser Scanning Microscope 510 META NLO, Zeiss, Germany) to observe living cells in green and dead cells in red.

Qualitative and quantitative valve tissue analyses

Histology and SEM

All TEHV (n=15) were evaluated qualitatively by histology. Representative pieces of TEHV were formalin-fixed and either embedded into paraffin and sectioned at 7 µm or snapfrozen and sectioned at 10 µm. The paraffin sections were stained with Haematoxylin and Eosin (H&E, Sigma-Aldrich) to visualize general tissue morphology and presence of cells, with Picrosirius Red for collagen structure, and with DAPI to assess the presence of cell nuclei. Frozen sections of the cell-populated and decellularized TEHV were stained with FITC-labeled phalloidin (1:200; Sigma-Aldrich) and DAPI to visualize (removal of) F-actin and nuclei, respectively. The H&E and Picrosirius Red staining were visualized by normal light microscopy. The Picrosirius Red staining was additionally visualized by polarized light

microscopy. DAPI and F-actin stainings were visualized by fluorescence microscopy. Tissue samples of the reseeded decellularized TEHV were fixed in 2% glutaraldehyde (Sigma, USA) and sputtered with platin in order to examine confluency of the seeded cells by SEM.

DNA and extracellular matrix analyses

Cell-populated (n=3), decellularized (n=4), and stored decellularized (n=2) TEHV were analyzed quantitatively for total amount of DNA, as an indicator for cell number, glycosaminoglycans, and hydroxyproline, as an indicator for collagen. For each valve, two samples per leaflet were analyzed. Hence, all valves contained 6 individual measurements, which were averaged to represent an average value for each valve. The amount of DNA was measured using the commercially available Quant-iT^{TM} Picogreen® dsDNA kit (Molecular Probes, Invitrogen). The glycosaminoglycans content was determined using a modified version of the protocol described by Farndale et al. [39] and a standard curve prepared from chondroitin sulphate from shark cartilage (Sigma Aldrich) in addition to the samples. Briefly, 40 µl of diluted sample (without addition of chondroitin AC lyase, chondroitin ABC lyase and keratanase) was pipetted into a 96-well plate in duplicate. Subsequently, 150 µl dimethylmethylene blue (46 µM dimethylmethylene blue, 40.5 mM glycin, 40.5 mM NaCl, pH 3.0) was added and absorbance was measured at 540 nm. Hydroxyproline content was determined according to the protocol described by Huszar et al. [40] and a standard curve prepared from trans-4-hydroxyproline (Sigma Aldrich). The amounts of DNA, glycosaminoglycans, and hydroxyproline were expressed per mg dry weight of tissue.

Mechanical analyses

The mechanical properties of the leaflets of cell-populated (n=3), decellularized (n=4), and stored decellularized (n=2) TEHV were determined by uniaxial tensile tests. Three strips in the circumferential and 4 strips in the radial direction (width=2.9±0.4mm) were cut from the leaflets from each TEHV. Stress-strain curves were obtained using a uniaxial tensile tester (Kammrath & Weiss GmbH, Dortmund Germany), equipped with a 20N load cell and all samples were tested at identical strain rate (150µm/s for strips 9 mm in length and 100µm/s for strips 6 mm in length). The ultimate tensile strength (UTS), as measure for tissue

strength, was defined as the maximum stress value in the stress-strain curve. The Youngs modulus, as measure for tissue stiffness, was determined as the slope in the linear region of the stress-strain curve at large strains. The obtained values for tissue strength and stiffness were averaged for each valve.

Statistics

Measurements are presented as the mean ± standard error of the mean (SEM). One-way ANOVA (post hoc Bonferroni) was used to determine the differences between the groups of valves with respect to functionality parameters, extracellular matrix contents and mechanical properties. STATGRAPHICS software (Statistical Graphics corp., USA) was used for statistical analysis with $p<0.05$ considered as statistically significant.

Results

Macroscopic valve appearance

The macroscopic appearance of the cell-populated TEHV revealed thin, shiny tissue formation in the wall and leaflets with no visual changes upon decellularization (Figure 1A, D, and G). After separation of the leaflets, the cell-populated TEHV demonstrated leaflet retraction (Figure 1B). In the decellularized TEHV and the MSC-reseeded decellularized TEHV retraction of the leaflets was minimal (Figure 1E and H, respectively). After exposure to pulmonary conditions in the valve tester for 20 minutes, the leaflets of the cell-populated TEHV had completely retracted (Figure 1C), while the decellularized leaflets did not show retraction after 24 hours of exposure to pulmonary conditions (Figure 1F). The crimping procedure to simulate minimally invasive valve delivery is demonstrated in Figure 1I.

In-vitro valve performance

Opening and closing behavior of the TEHV was improved after decellularization (Figure 2), though some prolapse of the leaflets was observed in the decellularized TEHV (Figure 2A).

In contrast, closure of the cell-populated valve leaflets was hampered by retraction of the leaflets (Figure 2B). The cell-populated TEHV demonstrated 30±9% regurgitation, which reduced by decellularization to 15±2% ($p<0.05$) and remained stable at 18±2% after 24 hours endurance testing. The effective orifice area (EOA, expressed in percentage of the valve root surface area) increased from 53±8% for the cell-populated TEHV to 66±3% for the decellularized TEHV ($p<0.05$). The EOA of the decellularized TEHV remained stable at 61±4% after 24 hours endurance testing. The peak systolic pressure gradient for the cell-populated TEHV was 17±2 mm Hg and was reduced to 10±1 mm Hg by decellularization ($p<0.05$), remaining stable at 8±1 mm Hg after 24 hours endurance testing. For comparison, the average values for the porcine aortic valve bioprothesis tested at similar conditions were 4±1% regurgitation and an EOA of 40±0% (both significantly lower compared to the decellularized TEHV, $p<0.05$). The peak systolic pressure gradient was 18±1 mm Hg (significantly higher compared to the decellularized TEHV, $p<0.05$).

Qualitative and quantitative valve tissue properties

Histological appearance

Histology of the cell-populated TEHV revealed cellular tissue formation (Figure 3A-C) with higher cellularity in the outer tissue layers, which was most clearly observed in the wall. Abundant amounts of cross-linked collagen were detected in the leaflets (Figure 3D and E) and the wall. After decellularization, no cells were detected (Figure 3F-H), while the structure and deposition of the collagen in the leaflets (Figure 3I and J) and the wall were maintained. Storage of the decellularized TEHV for 18 months did not affect the histological appearance (data not shown).

DNA and extracellular matrix

The results of the quantitative tissue analyses are presented in Figure 5. Decellularization of the TEHV revealed a significant reduction (over 99%) in the amount of DNA. Although the amount of glycosaminoglycans was significantly reduced after decellularization, no

differences with respect to the amount of hydroxyproline (representative for 10% of the amount of collagen [41]) were observed. Storage of the decellularized valves did not affect tissue matrix composition. Compared to native valves, the cell-populated TEHV showed 28% of the DNA amount, 74% of collagen amount, and 94% of the amount of glycosaminoglycans measured in native ovine valve leaflets [22].

Mechanical properties

No significant differences were observed in mechanical behavior of the strips in radial direction compared to circumferential direction in both the cell-populated and decellularized TEHV. Therefore, these values were pooled. The decellularized and stored decellularized TEHV showed a shift of the stress-strain curves to the left when compared to the cell-populated TEHV (Figure 5A). The Youngs modulus of the decellularized TEHV was increased compared to the cell-populated TEHV (Figure 5B). The decellularization procedure did not affect tissue strength (UTS), but reduced the thickness of the TEHV (Figure 5B). Storage of the decellularized TEHV for 18 months did not significantly change the mechanical properties compared to the decellularized TEHV (Figure 5B).

MSC characterization, differentiation, and reseeding of decellularized TEHV

The bone marrow derived population of cells exhibited an immunophenotype associated with cultured MSC (CD29+/CD44+/CD166+/ Stro-4+/CD14+-/CD45-/CD31-; data not shown). Moreover, differentiation potential of the cells was demonstrated by differentiation into osteogenic, chondrogenic, and adipogenic cell lineages (Figure 6A, B, and C, respectively). After reseeding the decellularized TEHV with MSC, a confluent layer of cells was demonstrated on the leaflets and wall by histology and SEM (Figure 6D-I).

Viability and crimping of reseeded decellularized TEHV

The confluent cell layer was demonstrated to consist of viable cells (Figure 7A), which remained viable after the simulated crimping procedure (Figure 7B), although some spots of local damage were observed (Figure 7B insert).

Discussion

In this study, we investigated the feasibility of a off-the-shelf tissue engineered homologous heart valve concept providing unrestricted availability and minimal risk for immunogenic reactions or disease transmission. Our approach was to decellularize in-vitro grown TEHV, based on rapidly degrading synthetic scaffolds, in order to create starter matrices for guided tissue generation and tissue engineering as an alternative to xeno-and homografts. Complete cell removal was demonstrated histologically and biochemically. The effects of decellularization on extracellular matrix content, biomechanical properties, and in-vitro valve functionality were assessed by comparisons to cell-populated TEHV. Further, the effect of storage on the tissue properties and the reseeding feasibility of the decellularized TEHV were evaluated as well as the potential of reseeded decellularized TEHV for minimally invasive valve delivery procedures.

Cell-mediated traction is functional in ensuring the development of a desirable, highly aligned extracellular matrix in tissue-engineered cardiovascular substitutes [23,26,32,42,43]. However, sustained traction forces can result in undesirable retraction of the leaflets, resulting in valvular regurgitation [12,19,22,24,26]. Although it has been suggested to avoid valvular insufficiency by creating longer leaflets and a larger coaptation areas [26,44], engineering bi-leaflet valves instead of tri-leaflet valves [23,44], or applying a biodegradable support material within the fibrin scaffold [19], a sustained solution to control these traction forces is still lacking. This study shows that decellularization of the TEHV effectively reduces the retraction of the leaflets in-vitro.

The efficiency of cell removal, as well as preservation of the matrix integrity is highly dependent on the decellularization method used. Cell remnant removal is necessary, as the presence of dead cells potentially lead to inflammation and or calcification in-vivo [45]. In the present study, we choose to decellularize our TEHV with sodium deoxycholate (SD). Various

studies showed that SD-based treatments are more efficient in cell removal, while maintaining matrix integrity and mechanical properties when compared to decellularization with Trypsin [8,46-48]. The use of SD is preferred above sodium dodecylsulfate (SDS) [8,49] and was used to produce xenogenic valve replacements that functioned properly in sheep [50]. Furthermore, an increased reseeding potential is documented for SD-treated extracellular matrix, when compared to SDS specimens [46]. The SD-treatment is often applied in combination with Triton X-100 [8,46], as decellularization using SD alone is not always satisfactory [50]. Therefore, we choose to include the use of Triton-X 100. The presence of small amounts of cellular antigens is described to be insufficient to elicit the type of pro-inflammatory or immune response that could adversely affect biological scaffold remodeling [51]. On the contrary, it is suggested that a low level expression of the α-gal-epitope has the potential to initiate an inflammatory response, leading to graft failure [9]. When translating the approach of the current study to human, the potential inflammatory response due to expression of the α-gal-epitope is avoided by using homologous cells. Nevertheless, with respect to calcification, complete cell removal should be pursued, as residual cells and cell remnants within the matrix might induce calcification [45]. The protocol used for decellularization of the TEHV in this study demonstrated to remove over 99% of the cellular material. Although serum nucleases can be applied to further reduce the DNA amounts in detergent pretreated tissues [29], the clinical efficacy of commercially available materials has been claimed despite small amounts of remaining DNA [51].

Preservation of collagen integrity in the decellularized valve replacements was demonstrated by histology. Remarkably, although not significant, biochemical analysis indicated a trend towards increased collagen amounts after decellularization, which has been observed previously by others [52]. This (non-significant) increase in collagen in the decellularized TEHV compared to the cell-populated TEHV is assumed to originate from the loss of cells and glycosaminoglycans, and therewith the relative decrease in the dry weight of the sample. In the current study, we observed a reduction of one-third of the amount of

glycosaminoglycans after decellularization. Although Grauss and colleagues [53] observed an almost complete washout of glycosaminoglycans after decellularization with Triton-X, most other studies investigating decellularization of biological matrices did not study the effect on glycosaminoglycans. Because glycosaminoglycans appear to play a significant role in shock absorption, tissue elasticity, and prevention of calcification [54], replenishment of the lost compounds should be pursued in-vivo to enhance valvular durability. As a mature elastic network has not yet been detected in our cell-populated TEHV, the effect of decellularization on the elastin network was not explored. However, the formation of an elastic network in the TEHV is of particular importance for the biomechanical behavior of the valve [55] and is subject of current research.

The decellularized valve leaflets were thinner compared to the cell-populated leaflets, which cause is twofold. Firstly, the observed reduction of glycosaminoglycans after decellularization is likely to be associated with a loss in water content. Secondly, the cell-populated leaflets were most probably thickened due to cell-mediated retraction directly after separation of the merged leaflets. The retraction in the cell-populated leaflets may also explain the observed shift to the left of the linear part of the stress-strain curve after decellularization. Similar shifts in stress-strain curves were observed for native decellularized tissues [28]. Elongation of the cell-populated samples before testing to their original length before retraction is hypothesized to result in the same shift as observed for the decellularized samples.

Tissue strength of the leaflets was not affected by the decellularization procedure. The tissue stiffness was increased, but did not negatively affect valve functionality of the decellularized TEHV. Moreover, peak systolic pressure gradients were decreased in the decellularized TEHV, while the EOA was increased, probably due to reduced thickness of the leaflets. Additionally, reduced leaflet retraction after decellularization had a beneficial effect on the regurgitation. Compared to the cell-populated TEHV, the decellularized TEHV showed significantly reduced regurgitation that remained stable up to 24 hours endurance testing.

Closure of the cell-populated TEHV was hampered by cell-mediated retraction of the leaflets and, therefore, endurance tests of these valves have not been performed. Although closure of the leaflets was significantly improved by decellularization, regurgitation was still observed, caused by subtle leaflet prolapse. Enlargement of the coaptation area of the leaflets is proposed to avoid the observed prolapse and is currently under investigation. The EOA and peak systolic pressure gradient of the decellularized TEHV were higher and lower, respectively, than those of the porcine aortic bioprosthesis. Though, it should be noted that the aortic bioprosthesis did not function satisfactory at pulmonary conditions.

Growth and remodeling of the valve replacement in-vivo requires a living tissue and, therewith, (re)population of the acellular tissue with cells. Still, it is unclear whether there is a need for recellularization prior to implantation, or whether circulating cells or cells from adjacent tissues may repopulate the scaffold in-vivo [56,57]. Engineered decellularized tissues may be superior for cellular migration compared to decellularized native tissues, due to a lack of prominent elastin barriers and a less mature collagen structure [28,52]. Long-term animal experiments have to clarify the need for in-vitro preseeding and are necessary to demonstrate growth and remodeling potential. Nevertheless, the feasibility of using decellularized TEHV as living implant was demonstrated by in-vitro reseeding with bone marrow derived mesenchymal stem cells (MSC). MSC are attractive candidates and successfully used to reseed decellularized matrices [11,58]. Moreover, MSC show a remarkable similarity in phenotype compared to valvular interstitial cells [59], demonstrate anti-thrombogenic [60], and immunosuppressive properties [61], and suitability for utilization in routine clinical practice, due to their ease of accessibility, handling and their use for multiple recipients [62]. Additionally, both the anti-thrombogenic properties of the MSC [60] and the ability to stimulate in-vivo endothelization [63] overcome the necessity of preseeding with endothelial cells.

After reseeding the decellularized TEHV, a confluent cell layer was observed within 3 days, without cell-mediated retraction of the leaflets. By reseeding the valves with MSC we aim for

in-vivo recellularization with recipient cells [64]. Reseeded or not, we hypothesize that leaflet retraction of the decellularized TEHV will not re-occur in-vivo, as the contractile myofibroblasts are removed and should be replaced by cells with a more quiescent and less contractile phenotype. Moreover, in-vivo leaflet shortening has been shown to be prevented by hemodynamic loading [65]. Nevertheless, animal experiments are mandatory to elucidate whether leaflet retraction will not re-occur in-vivo.

Storage of the valves for 18 months did not affect the collagen structure, extra cellular matrix composition or the mechanical behavior. These results support the potential use of decellularized TEHV to serve as off-the-shelf valve replacements. Besides, clinical application for guided tissue generation and tissue engineering is attractive as the decellularized TEHV are suitable for minimally invasive implantation techniques. These heart valve replacement procedures represent an attractive alternative treatment option for patients with valvular heart disease and will likely have a major impact on the management of these patients over the next several years [66]. A perquisite for minimally invasive implantation techniques is crimping of the valve to fit the delivery device. In the case of a living implant, the crimping could be harmful to the cells. Therefore, simulation of the necessitated crimping procedure was evaluated for the reseeded decellularized TEHV. The observed cell damage due this crimping procedure was small and only locally. Therefore, the crimping is hypothesized not to affect the proposed in-vivo recruitment of cells by the MSC.

Conclusion

Here we demonstrate that decellularization of TEHV is feasible with efficient cell removal and preservation of collagen and tissue strength. By creating TEHV from rapid degrading synthetic scaffolds and homologous cells we avoid the risks for xenograft-specific immune responses or disease transmission. Moreover, decellularization enables on-the-shelf storage of the in-vitro grown TEHV and strongly reduces cell-mediated retraction, thereby improving valve performance. Decellularized homologous TEHV have the potential to serve as largely

available off-the-shelf scaffolds without risk for xenogenic disease transmission. These scaffolds can be used as starter material for guided tissue generation and tissue engineering and potentially serve as an alternative to xeno-and homografts.

Acknowledgements

The authors thank Ms. Leonie Grootzwagers and Ms. Marloes Janssen - van den Broek (Department of Biomedical Engineering, TU/e) for help with cell and tissue culture, decellularization of the TEHV, ECM analyses, and FACS analyses. Moreover, the authors thank Benedikt Weber (Swiss Center for Regenerative Medicine, UHZ) for help with SEM analyses. The research leading to these results has received funding from the European Union's Seventh Framework Programme (FP7/2007-2013) under grant agreement n° 242008 and from the Dutch Program for Tissue Engineering (DPTE).

References

(1) Pibarot P, Dumesnil JG. Prosthetic heart valves: selection of the optimal prosthesis and long-term management. Circulation 2009;119(7):1034-48.

(2) Elkins RC, Dawson PE, Goldstein S, Walsh SP, Black KS. Decellularized human valve allografts. Ann Thorac Surg 2001;71(90050):S428-S432.

(3) Booth C, Korossis SA, Wilcox HE, Watterson KG, Kearney JN, Fisher J, et al. Tissue engineering of cardiac valve prostheses I: development and histological characterization of an acellular porcine scaffold. J Heart Valve Dis 2002;11(4):457-62.

(4) Cebotari S, Tudorache I, Ciubotaru A, Boethig D, Sarikouch S, Goerler A, et al. Use of fresh decellularized allografts for pulmonary valve replacement may reduce the reoperation rate in children and young adults: early report. Circulation 2011;124(11 Suppl):S115-S123.

(5) Konertz W, Angeli E, Tarusinov G, Christ T, Kroll J, Dohmen PM, et al. Right ventricular outflow tract reconstruction with decellularized porcine xenografts in patients with congenital heart disease. J Heart Valve Dis 2011;20(3):341-7.

(6) Dohmen PM, Lembcke A, Holinski S, Pruss A, Konertz W. Ten years of clinical results with a tissue-engineered pulmonary valve. Ann Thorac Surg 2011;92(4):1308-14.

(7) Badylak SF, Gilbert TW. Immune response to biologic scaffold materials. Semin Immunol 2008;20(2):109-16.

(8) Kasimir MT, Rieder E, Seebacher G, Silberhumer G, Wolner E, Weigel G, et al. Comparison of different decellularization procedures of porcine heart valves. Int J Artif Organs 2003;26(5):421-7.

(9) Kasimir MT, Rieder E, Seebacher G, Nigisch A, Dekan B, Wolner E, et al. Decellularization does not eliminate thrombogenicity and inflammatory stimulation in tissue-engineered porcine heart valves. J Heart Valve Dis 2006;15(2):278-86.

(10) Neuenschwander S, Hoerstrup SP. Heart valve tissue engineering. Transpl Immunol 2004;12(3-4):359-65.

(11) Iop L, Renier V, Naso F, Piccoli M, Bonetti A, Gandaglia A, et al. The influence of heart valve leaflet matrix characteristics on the interaction between human mesenchymal stem cells and decellularized scaffolds. Biomaterials 2009;30(25):4104-16.

(12) Shinoka T, Breuer CK, Tanel RE, Zund G, Miura T, Ma PX, et al. Tissue engineering heart valves: valve leaflet replacement study in a lamb model. Ann Thorac Surg 1995;60(6 Suppl):S513-S516.

(13) Mol A, van Lieshout MI, Dam-de Veen CG, Neuenschwander S, Hoerstrup SP, Baaijens FPT, et al. Fibrin as a cell carrier in cardiovascular tissue engineering applications. Biomaterials 2005;26(16):3113-21.

(14) Sutherland FWH, Perry TE, Yu Y, Sherwood MC, Rabkin E, Masuda Y, et al. From stem cells to viable autologous semilunar heart valve. Circulation 2005;111(21):2783-91.

(15) Engelmayr GC, Jr., Sales VL, Mayer JE, Jr., Sacks MS. Cyclic flexure and laminar flow synergistically accelerate mesenchymal stem cell-mediated engineered tissue formation: Implications for engineered heart valve tissues. Biomaterials 2006;27(36):6083-95.

(16) Hoerstrup SP, Sodian R, Daebritz S, Wang J, Bacha EA, Martin DP, et al. Functional living trileaflet heart valves grown in vitro. Circulation 2000;102(19 Suppl 3):III44-III49.

(17) Hoerstrup SP, Kadner A, Melnitchouk S, Trojan A, Eid K, Tracy J, et al. Tissue engineering of functional trileaflet heart valves from human marrow stromal cells. Circulation 2002;106(12 Suppl 1):I143-I150.

(18) Mol A, Rutten MC, Driessen NJ, Bouten CV, Zund G, Baaijens FP, et al. Autologous human tissue-engineered heart valves: prospects for systemic application. Circulation 2006;114(1 Suppl):I152-I158.

(19) Flanagan TC, Sachweh JS, Frese J, Schnoring H, Gronloh N, Koch S, et al. In vivo remodeling and structural characterization of fibrin-based tissue-engineered heart valves in the adult sheep model. Tissue Eng Part A 2009;15(10):2965-76.

(20) Gottlieb D, Kunal T, Emani S, Aikawa E, Brown DW, Powell AJ, et al. In vivo monitoring of function of autologous engineered pulmonary valve. J Thorac Cardiovasc Surg 2010;139(3):723-31.

(21) Lutter G, Metzner A, Jahnke T, Bombien R, Boldt J, Iino K, et al. Percutaneous tissue-engineered pulmonary valved stent implantation. Ann Thorac Surg 2010;89(1):259-63.

(22) Schmidt D, Dijkman PE, Driessen-Mol A, Stenger R, Mariani C, Puolakka A, et al. Minimally-invasive implantation of living tissue engineered heart valves: a comprehensive approach from autologous vascular cells to stem cells. J Am Coll Cardiol 2010;56(6):510-20.

(23) Robinson PS, Johnson SL, Evans MC, Barocas VH, Tranquillo RT. Functional tissue-engineered valves from cell-remodeled fibrin with commissural alignment of cell-produced collagen. Tissue Eng Part A 2008;14(1):83-95.

(24) Shinoka T, Ma PX, Shum-Tim D, Breuer CK, Cusick RA, Zund G, et al. Tissue-engineered heart valves. Autologous valve leaflet replacement study in a lamb model. Circulation 1996;94(9 Suppl):II164-II168.

(25) Vlimmeren MAv, Driessen-Mol A, Oomens CWJ, Baaijens FPT. An In Vitro Model System to Quantify Stress Generation, Compaction, and Retraction in Engineered Heart Valve Tissue. Tissue Eng Part C Methods 2011;17(10):983-991.

(26) Syedain ZH, Lahti MT, Johnson SL, Robinson PS, Ruth GR, Bianco RW, et al. Implantation of a Tissue-engineered Heart Valve from Human Fibroblasts Exhibiting Short Term Function in the Sheep Pulmonary Artery. Cardiovascular Engineering and Technology 2011;2(2):101-2.

(27) Gilbert TW, Sellaro TL, Badylak SF. Decellularization of tissues and organs. Biomaterials 2006;27(19):3675-83.

(28) Dahl SLM, Koh J, Prabhakar V, Niklason LE. Decellularized native and engineered arterial scaffolds for transplantation. Cell Transplant 2003;12(6):659-66.

(29) Gui L, Chan SA, Breuer CK, Niklason LE. Novel utilization of serum in tissue decellularization. Tissue Eng Part C Methods 2010;16(2):173-84.

(30) Dahl SLM, Kypson AP, Lawson JH, Blum JL, Strader JT, Li Y, et al. Readily available tissue-engineered vascular grafts. Sci Transl Med 2011;3(68):68ra9.

(31) Geemen Dv, Driessen-Mol A, Grootzwagers LGM, Soekhradj-Soechit RS, Riem Vis PW, Baaijens FPT, et al. Variation in Tissue Outcome of Ovine and Human Engineered Heart Valve Constructs: Relevance for Tissue Engineering. Regen Med 2012;7(1):59-70.

(32) Mol A, Driessen NJB, Rutten MCM, Hoerstrup SP, Bouten CVC, Baaijens FPT. Tissue engineering of human heart valve leaflets: a novel bioreactor for a strain-based conditioning approach. Ann Biomed Eng 2005;33(12):1778-88.

(33) Spina M, Ortolani F, El MA, Gandaglia A, Bujan J, Garcia-Honduvilla N, et al. Isolation of intact aortic valve scaffolds for heart-valve bioprostheses: extracellular matrix structure, prevention from calcification, and cell repopulation features. J Biomed Mater Res A 2003;67(4):1338-50.

(34) Ye X, Zhao Q, Sun X, Li H. Enhancement of mesenchymal stem cell attachment to decellularized porcine aortic valve scaffold by in vitro coating with antibody against CD90: a preliminary study on antibody-modified tissue-engineered heart valve. Tissue Eng Part A 2009;15(1):1-11.

(35) Geven MCF, Bohte VN, Aarnoudse WH, van den Berg PMJ, Rutten MCM, Pijls NHJ, et al. A physiologically representative in vitro model of the coronary circulation. Physiol Meas 2004;25(4):891-904.

(36) Pittenger MF, Mackay AM, Beck SC, Jaiswal RK, Douglas R, Mosca JD, et al. Multilineage potential of adult human mesenchymal stem cells. Science 1999;284(5411):143-7.

(37) Gronthos S, McCarty R, Mrozik K, Fitter S, Paton S, Menicanin D, et al. Heat shock protein-90 beta is expressed at the surface of multipotential mesenchymal precursor cells: generation of a novel monoclonal antibody, STRO-4, with specificity for mesenchymal precursor cells from human and ovine tissues. Stem Cells Dev 2009;18(9):1253-62.

(38) Breuls RGM, Mol A, Petterson R, Oomens CWJ, Baaijens FPT, Bouten CVC. Monitoring local cell viability in engineered tissues: a fast, quantitative, and nondestructive approach. Tissue Eng 2003;9(2):269-81.

(39) Farndale RW, Buttle DJ, Barrett AJ. Improved quantitation and discrimination of sulphated glycosaminoglycans by use of dimethylmethylene blue. Biochim Biophys Acta 1986;883(2):173-7.

(40) Huszar G, Maiocco J, Naftolin F. Monitoring of collagen and collagen fragments in chromatography of protein mixtures. Anal Biochem 1980;105(2):424-9.

(41) Piez K, Likins RC. The nature of collagen. In: Sognnaes, R.F. ed. Calcification in biological systems. A symposium presented at the Washington meeting of the American Association for the Advancement of Science, 1958. 1960 p. 411-20.

(42) Barocas VH, Girton TS, Tranquillo RT. Engineered alignment in media equivalents: magnetic prealignment and mandrel compaction. J Biomech Eng 1998;120(5):660-6.

(43) Shi Y, Vesely I. Fabrication of mitral valve chordae by directed collagen gel shrinkage. Tissue Eng 2003;9(6):1233-42.

(44) Neidert MR, Tranquillo RT. Tissue-engineered valves with commissural alignment. Tissue Eng 2006;12(4):891-903.

(45) Human P, Zilla P. Characterization of the immune response to valve bioprostheses and its role in primary tissue failure. Ann Thorac Surg 2001;71(5 Suppl):S385-S388.

(46) Rieder E, Kasimir MT, Silberhumer G, Seebacher G, Wolner E, Simon P, et al. Decellularization protocols of porcine heart valves differ importantly in efficiency of cell removal and susceptibility of the matrix to recellularization with human vascular cells. J Thorac Cardiovasc Surg 2004;127(2):399-405.

(47) Tudorache I, Cebotari S, Sturz G, Kirsch L, Hurschler C, Hilfiker A, et al. Tissue engineering of heart valves: biomechanical and morphological properties of decellularized heart valves. J Heart Valve Dis 2007;16(5):567-73.

(48) Baraki H, Tudorache I, Braun M, Hoffler K, Gorler A, Lichtenberg A, et al. Orthotopic replacement of the aortic valve with decellularized allograft in a sheep model. Biomaterials 2009;30(31):6240-6.

(49) Zhou J, Fritze O, Schleicher M, Wendel HP, Schenke-Layland K, Harasztosi C, et al. Impact of heart valve decellularization on 3-D ultrastructure, immunogenicity and thrombogenicity. Biomaterials 2010;31(9):2549-54.

(50) Erdbrugger W, Konertz W, Dohmen PM, Posner S, Ellerbrok H, Brodde OE, et al. Decellularized xenogenic heart valves reveal remodeling and growth potential in vivo. Tissue Eng 2006;12(8):2059-68.

(51) Gilbert TW, Freundb S JM, Badylak SF. Quantification of DNA in Biologic Scaffold Materials. J Surg Res 2009;152(1):135-9.

(52) Gui L, Muto A, Chan SA, Breuer CK, Niklason LE. Development of decellularized human umbilical arteries as small-diameter vascular grafts. Tissue Eng Part A 2009 Sep;15(9):2665-76.

(53) Grauss RW, Hazekamp MG, Oppenhuizen F, van Munsteren CJ, Gittenberger-de Groot AC, DeRuiter MC. Histological evaluation of decellularised porcine aortic valves: matrix changes due to different decellularisation methods. Eur J Cardiothorac Surg 2005;27(4):566-71.

(54) Simionescu DT, Lovekamp JJ, Vyavahare NR. Glycosaminoglycan-degrading enzymes in porcine aortic heart valves: implications for bioprosthetic heart valve degeneration. J Heart Valve Dis 2003;12(2):217-25.

(55) Mol A, Smits AI, Bouten CV, Baaijens FP. Tissue engineering of heart valves: advances and current challenges. Expert Rev Med Devices 2009;6(3):259-75.

(56) Simon P, Kasimir MT, Seebacher G, Weigel G, Ullrich R, Salzer-Muhar U, et al. Early failure of the tissue engineered porcine heart valve SYNERGRAFT in pediatric patients. Eur J Cardiothorac Surg 2003;23(6):1002-6.

(57) Miller DV, Edwards WD, Zehr KJ. Endothelial and smooth muscle cell populations in a decellularized cryopreserved aortic homograft (SynerGraft) 2 years after implantation. J Thorac Cardiovasc Surg 2006;132(1):175-6.

(58) Vincentelli A, Wautot F, Juthier F, Fouquet O, Corseaux D, Marechaux S, et al. In vivo autologous recellularization of a tissue-engineered heart valve: are bone marrow mesenchymal stem cells the best candidates? J Thorac Cardiovasc Surg 2007;134(2):424-32.

(59) Latif N, Sarathchandra P, Thomas PS, Antoniw J, Batten P, Chester AH, et al. Characterization of structural and signaling molecules by human valve interstitial cells and comparison to human mesenchymal stem cells. J Heart Valve Dis 2007;16(1):56-66.

(60) Hashi CK, Zhu Y, Yang GY, Young WL, Hsiao BS, Wang K, et al. Antithrombogenic property of bone marrow mesenchymal stem cells in nanofibrous vascular grafts. Proceedings of the National Academy of Sciences 2007;104(29):11915-20.

(61) Uccelli A, Moretta L, Pistoia V. Immunoregulatory function of mesenchymal stem cells. Eur J Immunol 2006;36(10):2566-73.

(62) Pittenger MF, Martin BJ. Mesenchymal stem cells and their potential as cardiac therapeutics. Circ Res 2004;95(1):9-20.

(63) Mirza A, Hyvelin JM, Rochefort GY, Lermusiaux P, Antier D, Awede B, et al. Undifferentiated mesenchymal stem cells seeded on a vascular prosthesis contribute to the restoration of a physiologic vascular wall. J Vasc Surg 2008;47(6):1313-21.

(64) Roh JD, Sawh-Martinez R, Brennan MP, Jay SM, Devine L, Rao DA, et al. Tissue-engineered vascular grafts transform into mature blood vessels via an inflammation-mediated process of vascular remodeling. Proc Natl Acad Sci U S A 2010;107(10):4669-74.

(65) Weber B, Scherman J, Emmert MY, Gruenenfelder J, Verbeek R, Bracher M, et al. Injectable living marrow stromal cell-based autologous tissue engineered heart valves: first experiences with a one-step intervention in primates. Eur Heart J 2011;32(22):2830-40.

(66) Rosengart TK, Feldman T, Borger MA, Vassiliades TAJ, Gillinov AM, Hoercher KJ, et al. Percutaneous and minimally invasive valve procedures: a scientific statement from the American Heart Association Council on Cardiovascular Surgery and Anesthesia, Council on Clinical Cardiology, Functional Genomics and Translational Biology Interdisciplinary Working Group, and Quality of Care and Outcomes Research Interdisciplinary Working Group. Circulation 2008;117(13):1750-67.

Figure legends

Figure 1: Macroscopic appearance of the cell-populated TEHV (A-C), decellularized (D-G), and reseeded TEHV (H-J). The macroscopic appearance of the cell-populated TEHV (A) was not affected by decellularization (D) and revealed thin, shiny tissue formation in the wall and leaflets (G; ventricular surface of the valve leaflets). Retraction of the leaflets of the cell-populated TEHV (B) is seen immediately after separation of the leaflets, which is absent in the decellularized TEHV (E) and did not re-occur after reseeding with MSC (H). After 20 minutes exposure to pulmonary conditions, the leaflets of the TEHV were completely retracted (C), while the decellularized leaflets do not show this retraction even after 24 hours of exposure to pulmonary conditions (F). In order to test their potential for minimally invasive implantation, the reseeded valves were crimped (I) before analyses.

Figure 2: In-vitro functionality of cell-populated and decellularized TEHV. (A) After decellularization the TEHV showed improved opening and closing behavior when exposed to pulmonary conditions, although some prolapse of the leaflets (indicated by black arrows) was observed. (B) Closure of the cell-populated valve leaflets was hampered by retraction of the leaflets.

Figure 3: Histology of the cell-populated (A-E) and decellularized (F-J) TEHV. Haematoxylin and Eosin staining (H&E; A, B, F, G), Phalloidin and DAPI staining (C and H), Picrosirius red staining visualized by transmitted light (D and I), and Picrosirius red staining visualized by polarized light (E and J). Overview of wall and leaflet of cell-populated TEHV (A) indicating locations of images B-E. Overview of wall and leaflet of decellularized TEHV (F) indicating locations of images G-J. Before decellularization, cellular tissues (A, B, and C) contained abundant amounts of collagen (D and E) and F-actin (C). After decellularization, the leaflets demonstrated preserved structural integrity (F and G) and collagen (I and J), but

no F-actin (H) or nuclei (F, G, and H). Scale bars in A and F represent 1 mm; Scale bars in B-E and G-J represent 200μm.

Figure 4: Amounts of glycosaminoglycans, hydroxyproline, and DNA in the leaflets of the cell-populated, decellularized, and stored decellularized TEHV. Values are represented as mean values ± SEM. The amount of DNA and glycosaminoglycans (GAG) was significantly reduced in the decellularized and stored decellularized TEHV compared to the cell-populated TEHV (**$p<0.01$ and *$p<0.05$, respectively). No differences with respect to the amount of hydroxyproline (Hyp; representative for 10% of the amount of collagen [41]) were observed in the decellularized and stored decellularized TEHV compared to the cell-populated TEHV. Storage of the decellularized TEHV did not affect the amounts of DNA, glycosaminoglycans (GAG), or hydroxyproline (Hyp).

Figure 5: Mechanical properties of the leaflets of the cell-populated, decellularized and stored decellularized TEHV. Values are represented as mean values ± SEM (A) Typical examples of stress-strain curves of uniaxial tensile tests. (B) Neither the decellularization procedure nor the storage period significantly affected the tissue strength (UTS) or stiffness (Youngs modulus). The thickness of the decellularized and stored decellularized TEHV was reduced compared to the cell-populated TEHV (* $p<0.05$).

Figure 6: MSC differentiation and reseeding of the decellularized TEHV. Differentiation potential of the MSC was demonstrated by differentiation into osteogenic (A*;* Alizarin Red S staining), chondrogenic (B; Toluidin blue staining), and adipogenic (C; Oil Red-O staining) cell lineages. After reseeding the decellularized TEHV, Haematoxylin and Eosin (D) and DAPI staining (E and F) confirmed the attachment of cells, which formed a confluent layer after 3 days, as demonstrated by SEM (G-I). Scale bars in: A and C represent 25μm; B represents 100μm; D-F represent 200μm; G-I represent 1mm, 100μm, and 10μm, respectively.

Figure 7: Viability of the reseeded decellularized TEHV before and after crimping. A confluent layer of living cells (green) was observed on the reseeded decellularized TEHV (A), which was still viable after crimping of the valves (B). Small clusters of dead cells (red, indicated by white arrows) were observed due to the crimping of the valves (enlarged in inserted image of B). Scale bars in A and B represent 200μm.

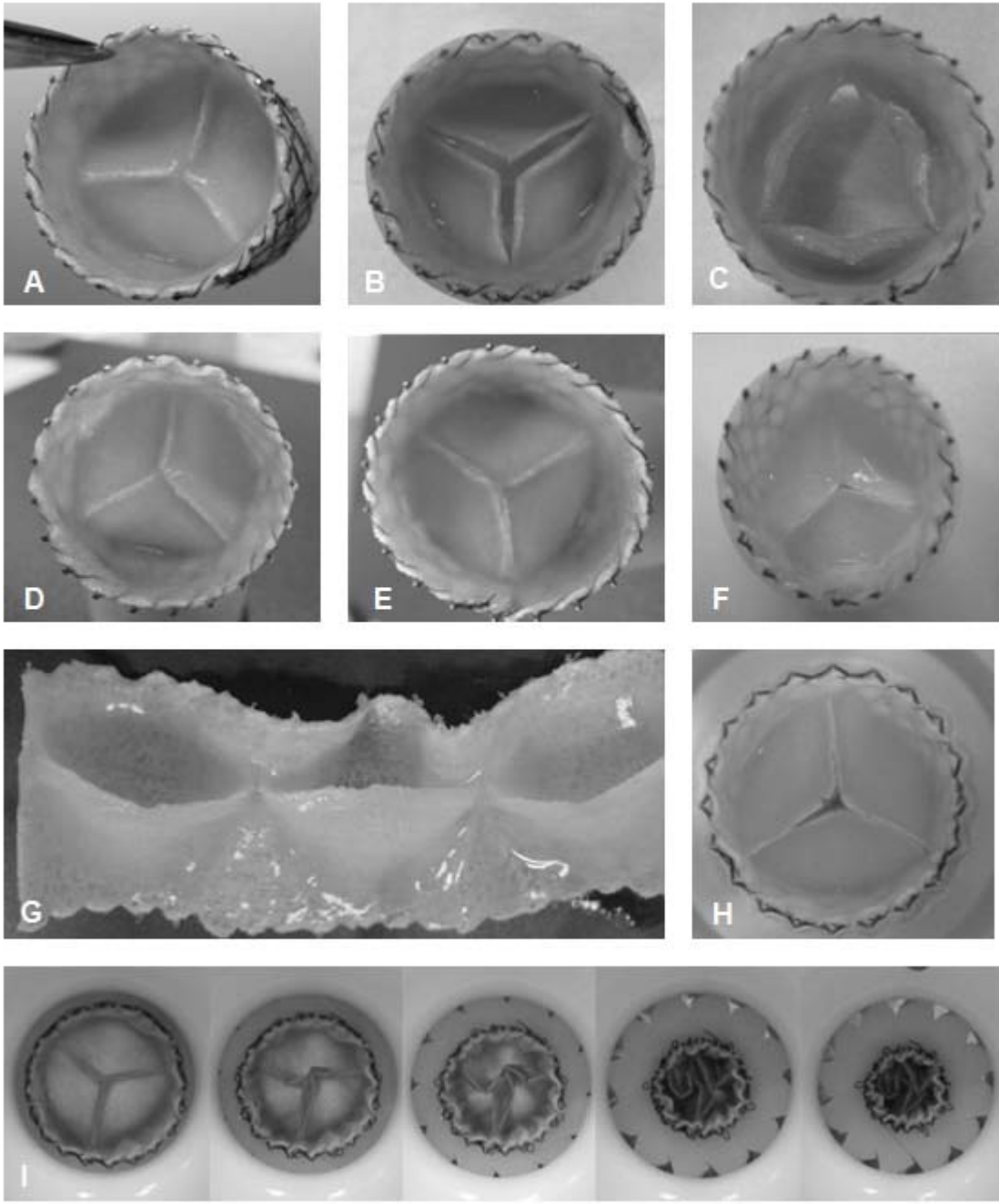
A
B
C
D
E
F
G
H
I

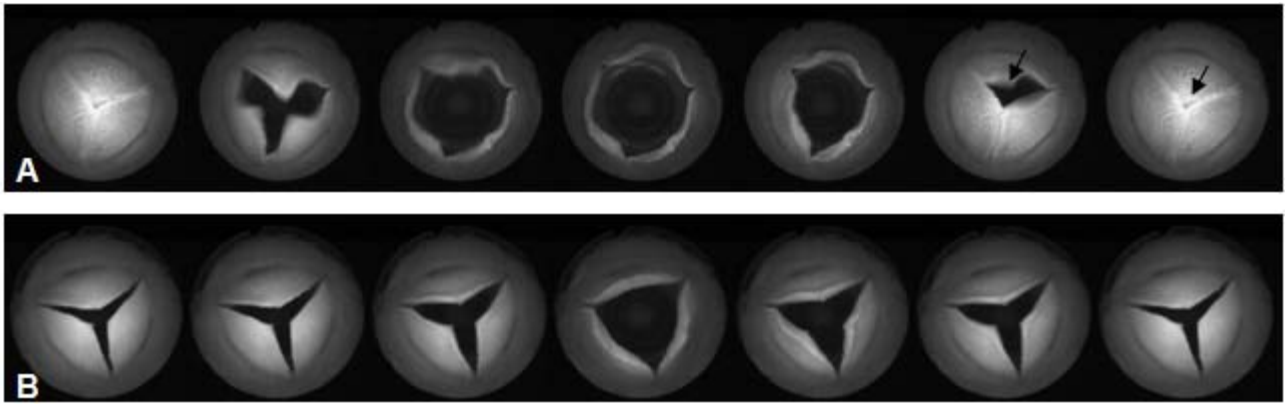
A
B

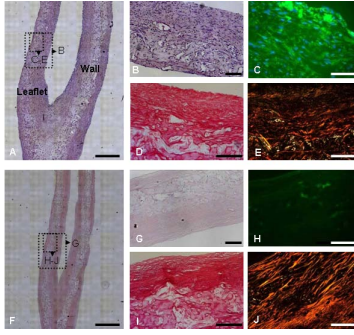
B
C
Wall
Leaflet
A
B
C
D
E
G
H
I
J

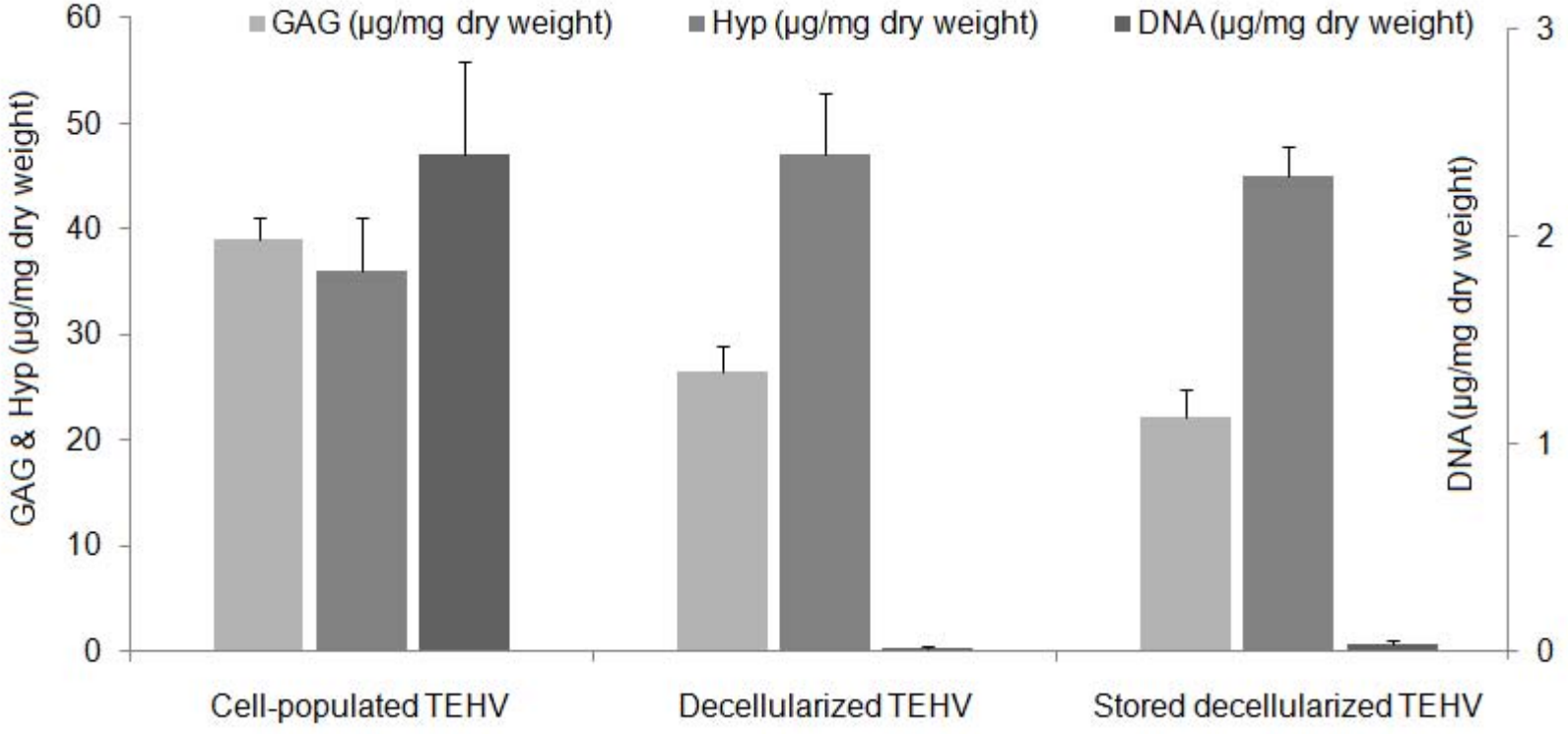
GAG (µg/mg dry weight)
Hyp (µg/mg dry weight)
DNA (µg/mg dry weight)
GAG & Hyp (µg/mg dry weight)
DNA (µg/mg dry weight)
60
50
40
30
20
10
0
3
2
1
0
Cell-populated TEHV
Decellularized TEHV
Stored decellularized TEHV

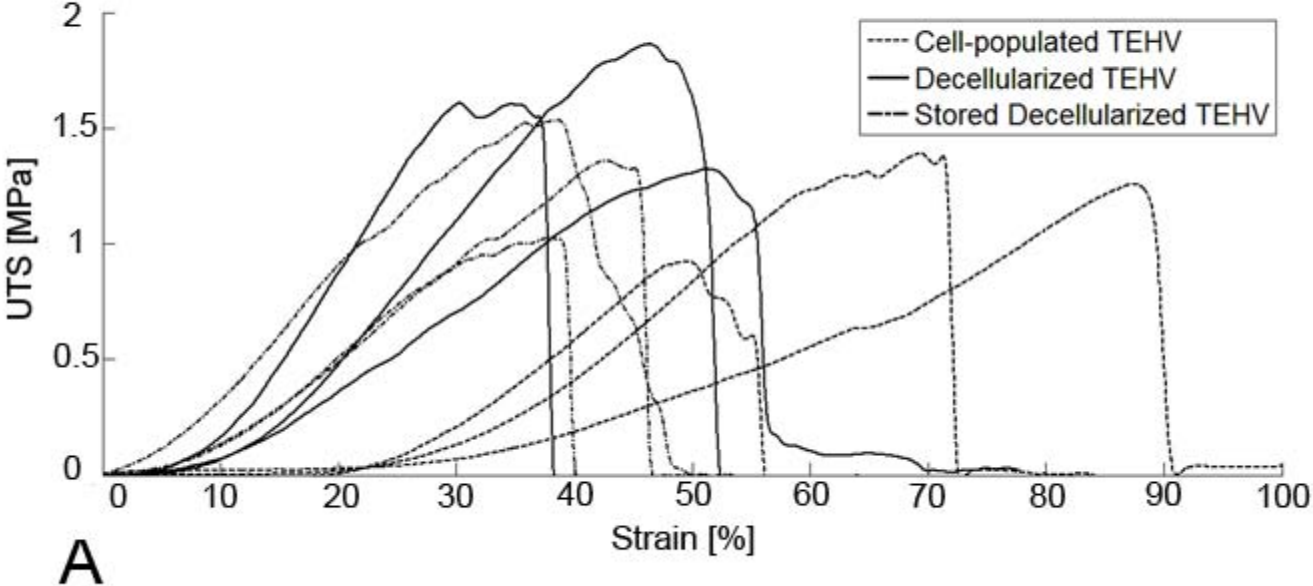
Cell-populated TEHV
Decellularized TEHV
Stored Decellularized TEHV
UTS [MPa]
Strain [%]
0
0.5
1
1.5
2
0
10
20
30
40
50
60
70
80
90
100
A

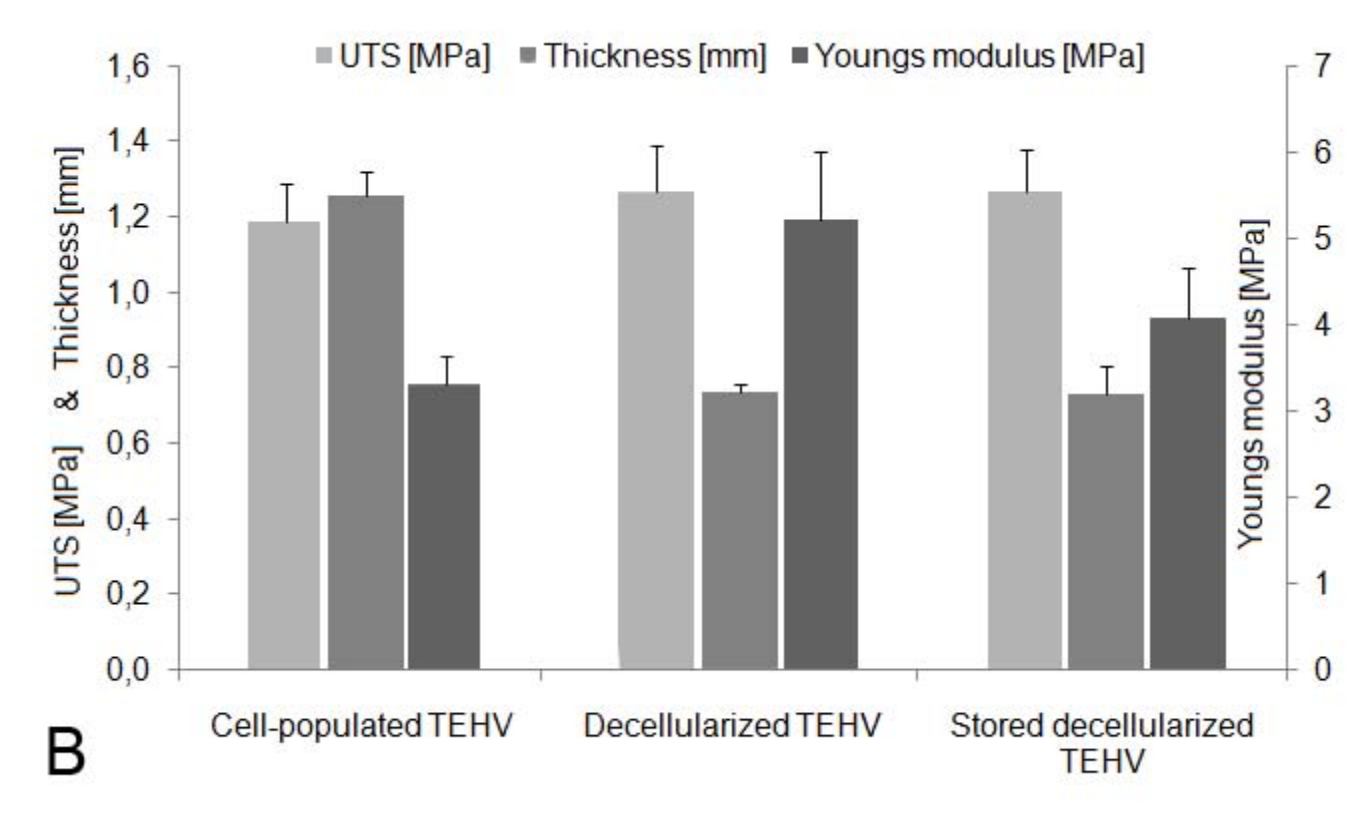
UTS [MPa]
Thickness [mm]
Youngs modulus [MPa]
UTS [MPa] & Thickness [mm]
Youngs modulus [MPa]
1,6
1,4
1,2
1,0
0,8
0,6
0,4
0,2
0,0
7
6
5
4
3
2
1
0
Cell-populated TEHV
Decellularized TEHV
Stored decellularized TEHV
B

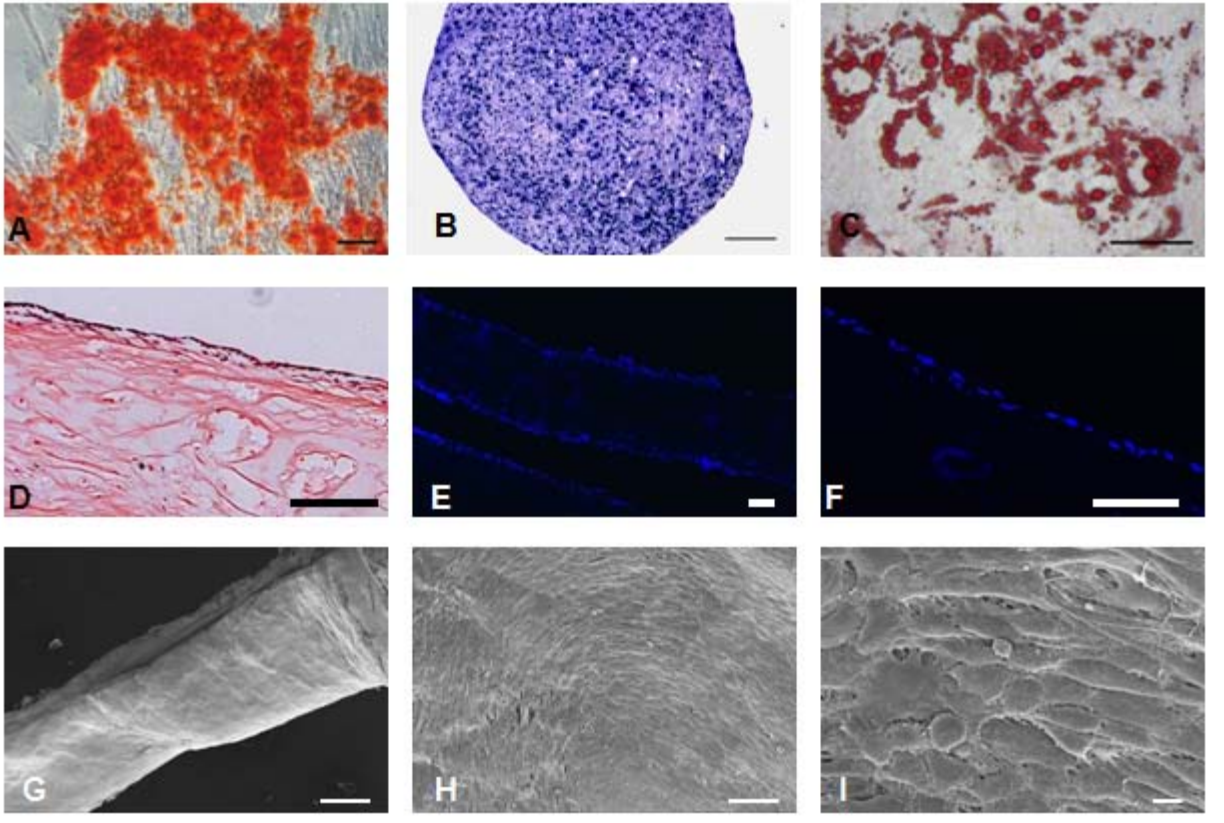
A
B
C
D
E
F
G
H
I

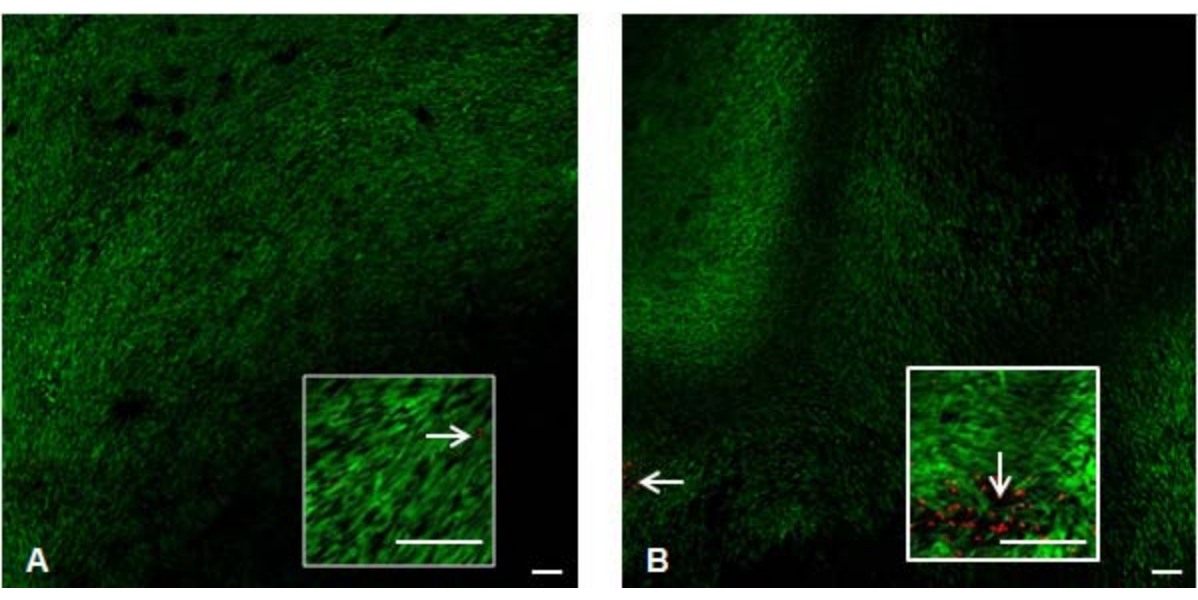
A
B